Journal of Applied Analysis and Computation
Volume 10, Number 2, April 2020, 795–815

Website:http://jaac-online.com/
DOI:10.11948/20190408

BIFURCATIONS AND EXACT TRAVELING WAVE SOLUTIONS OF THE EQUIVALENT COMPLEX SHORT-PULSE EQUATIONS

Jinsen Zhuang[1] and Yan Zhou[1,†]

Abstract In this paper, we study the traveling wave solutions for a complex short-pulse equation of both focusing and defocusing types, which governs the propagation of ultrashort pulses in nonlinear optical fibers. It can be viewed as an analog of the nonlinear Schrödinger (NLS) equation in the ultrashort-pulse regime. The corresponding traveling wave systems of the equivalent complex short-pulse equations are two singular planar dynamical systems with four singular straight lines. By using the method of dynamical systems, bifurcation diagrams and explicit exact parametric representations of the solutions are given, including solitary wave solution, periodic wave solution, peakon solution, periodic peakon solution and compacton solution under different parameter conditions.

Keywords Solitary wave solution, periodic wave solution, peakon solution, periodic peakon solution, compacton solution, equivalent complex short-pulse equation.

MSC(2010) 34C60, 35Q51, 35C05, 35C07, 35C08.

1. Introduction

Schäfer and Wayne [17] derived a short-pulse (SP) equation

$$u_{xt} = u + 16(u^3)_{xx}, \tag{1.1}$$

to describe the propagation of ultrashort optical pulses in nonlinear media. Here $u = u(x,t)$ is a real-valued function, representing the magnitude of the electric field; the subscripts t and x denote partial differentiation. The SP equation has been shown to be completely integrable (see [1, 2, 15]), whose periodic and loop solutions of the SP equation were studied in [6, 7, 12–14, 16].

Similar to the nonlinear Schröinger (NLS) equation, it is known that the complex valued function has advantages in describing optical waves which have both the amplitude and phase information [20]. Following this spirit, Feng [4] proposed the following complex short-pulse (CSP) equations:

$$q_{xt} \pm q + \frac{1}{2}\sigma(|q|^2 q_x)_x = 0, \tag{1.2}$$

†The corresponding author. Email address:zy4233@hqu.edu.cn(Y. Zhou)
[1]School of Mathematical Sciences, Huaqiao University, Quanzhou, Fujian 362021, China
*This research was partially supported by the National Natural Science Foundation of China (Nos. 11871231 and 11162020).

where $\sigma = \pm 1$ (also see [18]). These equations can be viewed as an analog of the NLS equation in the ultrashort-pulse regime when the width of optical pulse is of the order 10^{-15}s. The NLS equation has the focusing and defocusing cases, which admits the bright- and dark-type soliton solutions, respectively. Therefore it is natural that the CSP equation can also have the focusing and defocusing type, for which $\sigma = 1$ represents the focusing case, and $\sigma = -1$ stands for the defocusing case.

More recently, Feng et al. [5] considered the following normalized wave equations:

$$E_{zz} - E_{tt} = \pm E + (|E|^2 E)_{tt}, \tag{1.3}$$

which are equivalent to the general complex short-pulse equations (1.2), by using some variable transformations (see [5]).

Let

$$E(z,t) = A(\xi)e^{i\phi(z,t)}, \quad \xi = z - vt, \quad \phi(z,t) = \omega(t - vz) + F(\xi). \tag{1.4}$$

Inserting this ansatz into (1.3) and making the variable transformation $\psi = \frac{vA}{\sqrt{1-v^2}}$, for the focusing case, Feng, et al. [5] obtained the following equation:

$$\psi_{\xi\xi} - \frac{6\psi\psi_\xi^2}{1-3\psi^2} - \frac{\omega^2\psi}{v^2(1-3\psi^2)}\left(\delta - \frac{\psi^2(4(1-\psi^2)^2 - \psi^2)}{4(1-\psi^2)^3}\right) = 0 \tag{1.5}$$

and

$$F(\xi) = -\frac{\omega}{2v}\int_{\xi_0}^{\xi} \frac{\psi^2(3-2\psi^2)d\xi}{1-\psi^2}, \tag{1.6}$$

where $\delta = \frac{v^2}{\omega^2(1-v^2)} - v^2$.

For the defocusing case, the equation becomes

$$\psi_{\xi\xi} - \frac{6\psi\psi_\xi^2}{1-3\psi^2} - \frac{\omega^2\psi}{v^2(1-3\psi^2)}\left(\frac{4(1-\psi^2)^2 - \psi^4}{4(\psi^2-1)^3} - \alpha\right) = 0, \tag{1.7}$$

$$F(\xi) = \frac{\omega}{2v}\int_{\xi_0}^{\xi} \frac{\psi^2(2\psi^2-3)d\xi}{(\psi^2-1)^2} + C_1\xi, \tag{1.8}$$

where $\alpha = v^2 - 1 - \frac{v^2}{\omega^2(v^2-1)} = -(1+\delta), C_1$ is an integral constant and we take the integral constant $C_0 = 0$ in the formula (38) of [5].

It is easy to see that equations (1.5) and (1.7) are equivalent to the planar dynamical systems:

$$\frac{d\psi}{d\xi} = y, \quad \frac{dy}{d\xi} = \frac{6\psi y^2}{1-3\psi^2} + \frac{\beta\psi}{(1-3\psi^2)}\left(\delta - \frac{\psi^2(4(1-\psi^2)^2-\psi^2)}{4(1-\psi^2)^3}\right) \tag{1.9}$$

and

$$\frac{d\psi}{d\xi} = y, \quad \frac{dy}{d\xi} = \frac{6\psi y^2}{1-3\psi^2} - \frac{\beta\psi}{(1-3\psi^2)}\left(\frac{4(1-\psi^2)^2-\psi^4}{4(1-\psi^2)^3} + \alpha\right), \tag{1.10}$$

where $\beta = \frac{\omega^2}{v^2} > 0$.

Clearly, systems (1.9) and (1.10) are two singular traveling wave systems of the first class defined in [8, 10] with a singular straight lines $\psi = \pm 1$ and $\psi = \pm\frac{1}{\sqrt{3}} = \pm\psi_s$, respectively.

Systems (1.9) and (1.10) have the first integrals, respectively, as follows:

$$\begin{aligned} H_+(\psi, y) =& y^2(1-3\psi^2)^2 + \frac{1}{2}\beta\Bigg[3(1+\delta)\psi^4 + \left(\frac{5}{2} - 2\delta\right)\psi^2 \\ &+ \frac{(1+\psi^2)}{4(1-\psi^2)^2} - \frac{13}{4(1-\psi^2)}\Bigg] = h \end{aligned} \tag{1.11}$$

and

$$\begin{aligned} &H_-(\psi, y) \\ =& y^2(1-3\psi^2)^2 + \frac{1}{2}\beta\left[-3\alpha\psi^4 + \left(\frac{9}{2} - 2\alpha\right)\psi^2 + \frac{(1+\psi^2)}{4(1-\psi^2)^2} - \frac{13}{4(1-\psi^2)}\right] \\ =& y^2(1-3\psi^2) + \frac{1}{2}\beta\left[3(1+\delta)\psi^4 + \left(\frac{13}{2} + 2\delta\right)\psi^2 + \frac{(1+\psi^2)}{4(1-\psi^2)^2} - \frac{13}{4(1-\psi^2)}\right] = h. \end{aligned} \tag{1.12}$$

We see from (1.11) and (1.12) that their difference is only in the coefficients of the term ψ^2.

Because the authors in [5] did not study the dynamical behavior and exact solutions for system (1.9) and (1.10) depending on the change of parameters of systems. In this paper, we use dynamical system method developed by [8–11] to investigate the solutions of system (1.9) and (1.10). We show that there exist solitary wave solutions, periodic wave solutions, peakon solutions, periodic peakon solutions and compacton solutions of systems (1.9) and (1.10), under different parameter conditions. We derive all possible exact explicit solutions for system (1.9). The main results are stated in Theorems 3.1-3.3 below.

From the analysis of bifurcations, we show that for the focusing and defocusing cases, the existence of solitary wave solutions, periodic wave solutions, peakon solutions, periodic peakon solutions and compacton solutions is similar. The difference is only in the parameter regions with respect to δ and α.

This paper is organized as follows. In Section 2, for a fixed $\beta > 0$, bifurcations of the phase portraits of system (1.9), depending on the changes of parameter δ, are discussed. In Section 3, classification of the traveling wave solutions of system (1.9) is given, with all possible explicit exact parametric representations of solutions for system (1.9). In Section 4, for a fixed $\beta > 0$, bifurcations of the phase portraits of system (1.10), depending on the changes of parameter α, are discussed.

2. Bifurcations of phase portraits of system (1.9)

In this section, we investigate the dynamical behavior of solutions of system (1.9). We first consider the associated regular system of system (1.9) as follows:

$$\begin{aligned} \frac{d\psi}{d\zeta} &= 4y(1-3\psi^2)(1-\psi^2)^3, \\ \frac{dy}{d\zeta} &= 24\psi y^2(1-\psi^2)^3 + \beta\psi[4\delta(1-\psi^2)^3 - \psi^2(4(1-\psi^2)^2 - \psi^2)], \end{aligned} \tag{2.1}$$

where $d\xi = 4(1-3\psi^2)(1-\psi^2)^3 d\zeta$. This system has the same first integral as (1.11). For system (2.1), the straight lines $\psi = \pm\frac{1}{\sqrt{3}}$ and $\psi = \pm 1$ is its four solutions.

Clearly, system (2.1) has an equilibrium point $E_0(0,0)$. For the other equilibrium points $E_j(\psi_j, 0)$ of system (2.1), $Z = Z_j = \psi_j^2$ satisfies the algebraic equation $f(Z) = 4\delta(1-Z)^3 - Z(4(1-Z)^2 - Z) = 4(1+\delta)Z^3 - 3(3+4\delta)Z^2 + 4(1+3\delta)Z - 4\delta = 0$, where $Z = \psi^2$. When $\delta \neq -1$, the function $f'(Z)$ has two zeros at $\hat{Z}_1 = \frac{9+12\delta-\sqrt{33+24\delta}}{12(1+\delta)}$ and $\hat{Z}_2 = \frac{9+12\delta+\sqrt{33+24\delta}}{12(1+\delta)}$. It is easy to see that

$$f(\hat{Z}_1) = \frac{1}{72(1+\delta)^2}\left[-(27+108\delta+72\delta^2) + (11+8\delta)\sqrt{33+24\delta}\right],$$

$$f(\hat{Z}_2) = -\frac{1}{72(1+\delta)^2}\left[(27+108\delta+72\delta^2) + (11+8\delta)\sqrt{33+24\delta}\right].$$

If and only if $\delta = -\frac{1}{54}(19+13\sqrt{13})$ or $\delta = \frac{1}{54}(-19+13\sqrt{13})$, we have $f(\hat{Z}_1) = 0$. Thus, when $\delta < -\frac{1}{54}(19+13\sqrt{13})$, or $\delta > \frac{1}{54}(-19+13\sqrt{13})$, $f(Z)$ only has one real positive zero. When $-\frac{1}{54}(19+13\sqrt{13}) < \delta < \frac{1}{54}(-19+13\sqrt{13})$, $f(Z)$ has three positive real zeros.

In the singular straight line $\psi = \pm\frac{1}{\sqrt{3}} = \pm\psi_s$, if $\delta \leq \frac{13}{32}$, there exist two equilibrium points $E_{s\pm}(\pm\psi_s, \pm Y_s)$ of system (2.1), respectively, where $Y_s = \frac{1}{6}\sqrt{6\beta(\frac{13}{32}-\delta)}$. Notice that $E_{s\pm}$ are not equilibrium points of system (1.9).

Let $M(\psi_j, y_j)$ be the coefficient matrices of the linearized systems of (1.9) at equilibrium point E_j and $J(\psi_j, y_j) = \det M_{\pm}(\phi_j, y_j)$. Then, one has

$$J(0,0) = -4\beta\delta, \quad J(\psi_s, Y_s) = -\frac{512}{729}\sqrt{6\beta\left(\frac{13}{32}-\delta\right)},$$

$$\begin{aligned} J(\psi_j, 0) = \beta\,\big[&-4\delta + 12(1+5\delta)\psi_j^2 - (117+324\delta)\psi_j^4 + (442+860\delta)\psi_j^6 - (828+1260\delta)\psi_j^8 \\ &+ (822+1044\delta)\psi_j^{10}) - (415+460\delta)\psi_j^{12} + 84(1+\delta)\psi_j^{14}\big]. \end{aligned}$$

According to the basic theory of planar dynamical systems, for an equilibrium point of a planar integrable system, if $J < 0$, then the equilibrium point is a saddle point; if $J > 0$, then it is a center point; if $J = 0$ and the Poincaré index of the equilibrium point is zero, then it is cusped.

For $H_+(\psi, y) = h$ given by (1.11), write

$$h_0 = H_+(0,0) = -\frac{3}{2}\beta, \quad h_s = H_+(\psi_s, Y_s) = -\frac{1}{48}\beta(71+8\delta), \quad h_j = H_+(\psi_j, 0).$$

Obviously, if and only if $\delta = \frac{1}{8}$, we have $h_0 = h_s$.

Without loss of generality, we assume that $\beta = \frac{\omega^2}{v^2}$ is a fixed positive real number. Then, by using the above information to do qualitative analysis, we obtain the bifurcations of phase portraits of system (1.9) shown in Figure 1(a)-(k).

We notice that the vector fields defined by (2.1) and (1.9) are different. The equilibrium points in the singular straight lines of system (2.1) are not equilibrium points of system (1.9). If along a heteroclinic loop of system (2.1), we make the variable ξ vary, such that the phase point passes through a singular straight line, then the direction of vector fields defined by (1.9) changes to the opposite direction defined by (2.1). Therefore, the large heteroclinic loop of system (2.1) enclosing

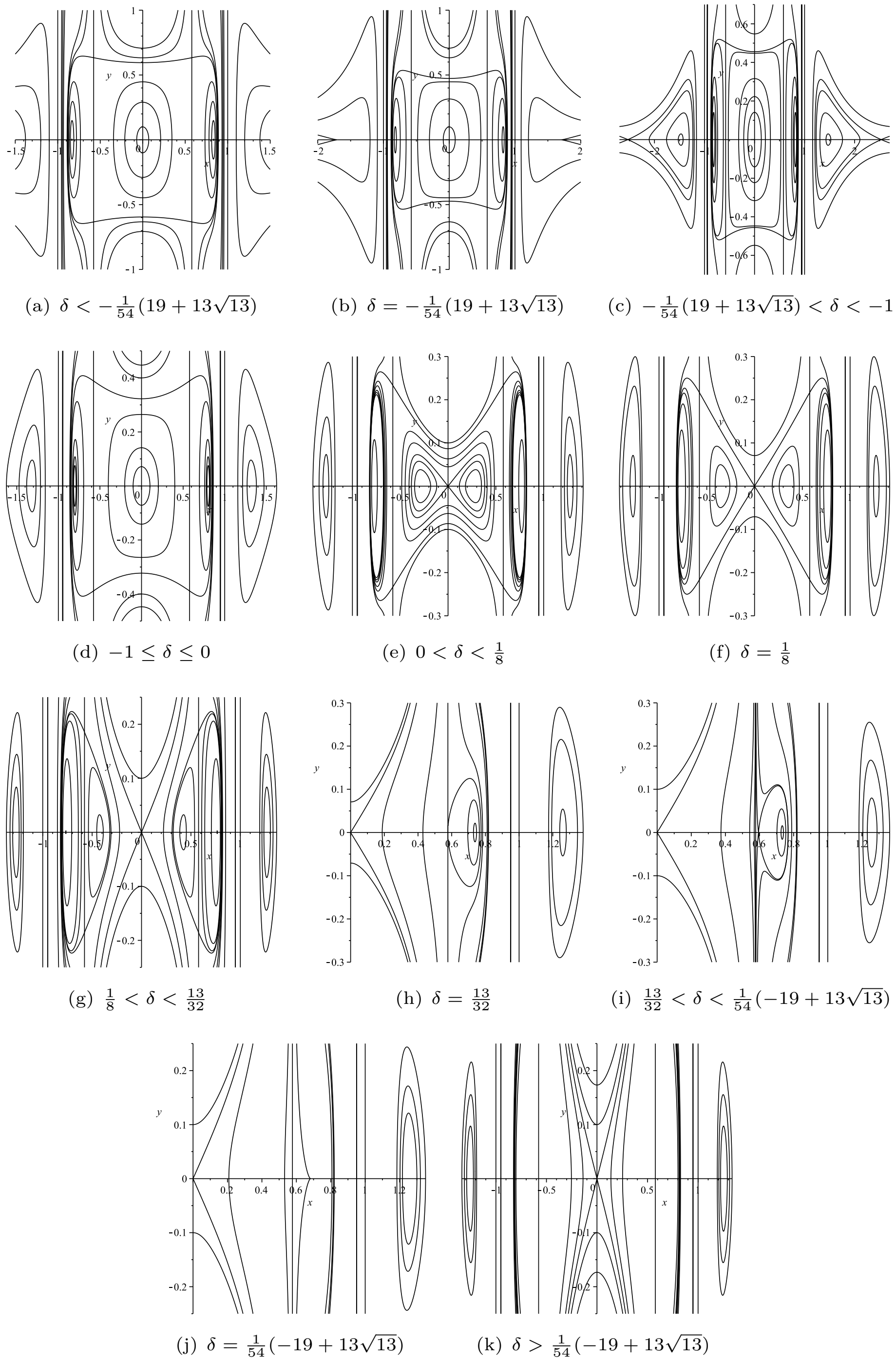

(a) $\delta < -\frac{1}{54}(19+13\sqrt{13})$ (b) $\delta = -\frac{1}{54}(19+13\sqrt{13})$ (c) $-\frac{1}{54}(19+13\sqrt{13}) < \delta < -1$

(d) $-1 \leq \delta \leq 0$ (e) $0 < \delta < \frac{1}{8}$ (f) $\delta = \frac{1}{8}$

(g) $\frac{1}{8} < \delta < \frac{13}{32}$ (h) $\delta = \frac{13}{32}$ (i) $\frac{13}{32} < \delta < \frac{1}{54}(-19+13\sqrt{13})$

(j) $\delta = \frac{1}{54}(-19+13\sqrt{13})$ (k) $\delta > \frac{1}{54}(-19+13\sqrt{13})$

Figure 1. Bifurcations of phase portraits of system (1.9) in the (ψ, y)-phase plane for a fixed $\beta > 0$

three equilibrium points in Figure 1(a)-(d) gives rise to a periodic solution of system (1.9). The large heteroclinic loop of system (2.1) enclosing two equilibrium points in Figure 1(f) can be see a homoclinic orbit of system (1.9), which gives rise to a solitary wave solution of system (1.9).

3. Classification of solutions $\psi(\xi)$ of system (1.9) and exact explicit parametric representations

In this section, we discuss the classification of the solutions $\psi(\xi)$ of system (1.9) and give possible exact explicit solutions. We see from (1.11) that for a fixed constant h,

$$\begin{aligned} y^2 &= \frac{4h(1-\psi^2)^2-\frac{1}{2}\beta[4(1-\psi^2)^2(3(1+\delta)\psi^4+(\frac{5}{2}-2\delta)\psi^2)+14\psi^2-12]}{4(1-3\psi^2)^2(1-\psi^2)^2} \\ &= \frac{(4h+24\beta)+(-8h-81\beta+4\beta\delta)\psi^2+(4h+84\beta-14\beta\delta)\psi^4+(-21\beta+16\beta\delta)\psi^6-6\beta(1+\delta)\psi^8}{4(1-3\psi^2)^2(1-\psi^2)^2} \\ &\equiv \frac{3\beta|1+\delta|G(\psi^2)}{2(1-3\psi^2)^2(1-\psi^2)^2}. \end{aligned} \tag{3.1}$$

Obviously, function $G(\psi^2)$ is a polynomial of degree eight with respect to ψ. By using the first equation of system (1.9), we have

$$\sqrt{6\beta|1+\delta|}\xi = \int_{\psi_0}^{\psi}\sqrt{\frac{4(1-3\psi^2)^2(1-\psi^2)^2}{G(\psi^2)}}d\psi = \int_{z_0}^{z}\frac{|(1-3z)(1-z)|}{\sqrt{z|G(z)|}}dz. \tag{3.2}$$

Clearly, the right hand of (3.2) is a hyperelliptic integral. Generally, we can not get the explicit exact solution from (3.2). Only in some special parametric conditions, we can obtain the parametric representations for the orbits shown in Figure 1.

3.1. Exact solitary wave solutions and peakon solutions determined by system (1.9)

It is well known that corresponding to a homoclinic orbit of system (1.9), there exists a solitary wave solutions of system (1.9). We see from Figure 1 that the level curves defined by $H_+(\psi, y) = h$ which contain two symmetric homoclinic orbits with respect to $y-$axis can be shown in Figure 2(a)-(d).

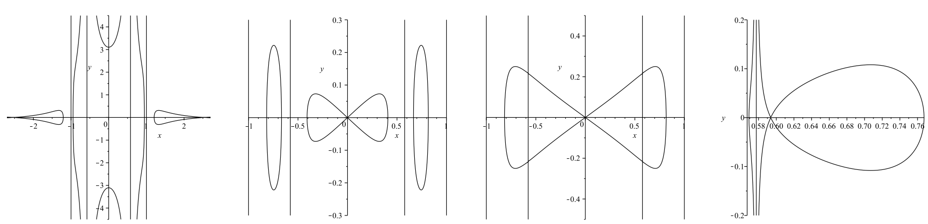

(a) $-\frac{1}{54}(19+13\sqrt{13}) < \delta < -1, h = h_3$. (b) $0 < \delta < \frac{1}{8}, h = h_0$. (c) $\delta = \frac{1}{8}, h = h_0 = h_s$. (d) $\frac{13}{32} < \delta < \frac{1}{54}(-19+13\sqrt{13}), h = h_1$.

Figure 2. Some level curves of system (1.9) defined by $H_+(\psi, y) = h$

(i) The case of $-\frac{1}{54}(19+13\sqrt{13}) < \delta < -1$ (see Figure 2(a)). The level curves defined by $H_+(\psi, y) = h_3$ contain two homoclinic orbits to the equilibrium point

$E_3(\psi_3, 0)$ and its symmetric point with respect to $y-$axis, two open stable manifolds and unstable manifolds of $E_3(\psi_3, 0)$ and its symmetric point, as well as four open curves which tend to the singular straight line $\psi = \pm\frac{1}{\sqrt{3}}$ when $|y| \to \infty$.

Corresponding to the right homoclinic orbit, the function $G(\psi^2) = (\psi_3^2 - \psi^2)^2(\psi^2 - \psi_m^2)(\psi^2 - \psi_l^2)$ in (3.2). Now, (3.2) can be written as

$$\sqrt{6\beta|1+\delta|}\xi = \int_{z_m}^{z} \frac{(3z-1)(z-1)dz}{(z_3-z)\sqrt{(z-z_m)(z-z_l)z}},$$

where $z_m = \psi_m^2, z_3 = \psi_3^2, z_l = \psi_l^2$. Thus, we obtain the following parametric representation of the dark solitary wave solution:

$$\begin{aligned}
\psi(\chi) &= \left(\psi_l^2 + \frac{\psi_m^2 - \psi_l^2}{\mathrm{cn}^2(\chi, k)}\right)^{\frac{1}{2}}, \quad \chi \in (0, \chi_{01}), \quad \chi \in (-\chi_{01}, 0), \quad \text{respectively},\\
\xi(\chi) =& \frac{2}{\psi_m\sqrt{6\beta|1+\delta|}}\left[\left((4-3(\psi_3^2-\psi_m^2)) + \frac{(3\psi_3^2-1)(\psi_3^2-1)}{\psi_3^2-\psi_l^2}\right)\chi\right.\\
&\pm 3\psi_m^2 E(\arcsin(\mathrm{sn}(\chi,k)),k) \mp 3\psi_m^2\mathrm{dn}(\chi,k)\mathrm{tn}(\chi,k)\\
&\left.\pm\frac{(3\psi_3^2-1)(\psi_3^2-1)(\psi_m^2-\psi_l^2)}{(\psi_3^2-\psi_l^2)(\psi_3^2-\psi_m^2)}\Pi\left(\arcsin(\mathrm{sn}(\chi,k)), \frac{\psi_3^2-\psi_l^2}{\psi_3^2-\psi_m^2}, k\right)\right],
\end{aligned} \tag{3.3}$$

where $k^2 = \frac{\psi_l^2}{\psi_m^2}$, $\chi_{01} = \mathrm{cn}^{-1}\left(\sqrt{\frac{\psi_m^2-\psi_l^2}{\psi_3^2-\psi_l^2}}, k\right)$, $\mathrm{sn}(u,k), \mathrm{cn}(u,k)$ and $\mathrm{dn}(u,k)$ are Jacobin elliptic functions, $E(\cdot,k), \Pi(\cdot,\cdot,k)$ are the incomplete elliptic integrals of the second kind and third kind (see [3]).

By the symmetry, letting $\psi \to -\psi$ in (16), we easily obtain the parametric representation of the bright solitary wave solution of system (1.9). Figure 3(a) and (b) show the profiles of two solitary waves.

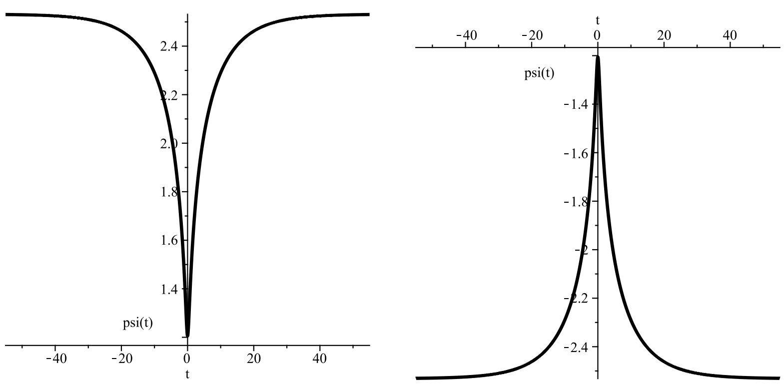

(a) Dark soliton (b) Bright soliton

Figure 3. Two solitary wave solutions of system (1.9) given by $H_+(\psi, y) = h_3$ when $\delta = -1.12$

Because there exist two segments of homoclinic orbits of system (1.9) defined by $H_+(\psi, y) = h_3$ which are close to two singular straight lines $\psi = \pm 1$. On the basis of the rapid-jump property of the derivative near the singular straight line given by [10], two solitary wave solutions shown in Figure 3(a) and (b) are two quasi-peakon solutions, for which the wave variable has two "time scales" (see [11]).

(ii) The case of $0 < \delta < \frac{1}{8}$ (see Figure 2(b)). The level curves defined by $H_+(\psi, y) = h_0$ contain two homoclinic orbits with eight figure to the equilibrium point $E_0(0,0)$, enclosing the equilibrium point $E_2(\psi_1, 0)$ and its symmetric point with respect to $y-$axis, as well as two periodic orbits enclosing the equilibrium point $E_2(\psi_2, 0)$ and its symmetric point with respect to $y-$axis (see Figure 2(b)).

Corresponding to the right homoclinic orbits, the function $G(\psi^2) = (r_1^2 - \psi^2)(r_2^2 - \psi^2)(\psi_M^2 - \psi^2)\psi^2$ in (3.2). Now (3.2) can be written as

$$\sqrt{6\beta|1+\delta|}\xi = \int_z^{z_M} \frac{(1-3z)(1-z)dz}{z\sqrt{(z_1-z)(z_2-z)(z_M-z)}},$$

where $z_M = \psi_M^2, z_1 = r_1^2, z_2 = r_2^2$. Thus, we obtain the following parametric representation of the bright solitary wave solution:

$$\begin{aligned}
\psi(\chi) &= \left(r_2^2 - \frac{r_2^2 - \psi_M^2}{\mathrm{cn}^2(\chi, k)}\right)^{\frac{1}{2}}, \qquad \chi \in (0, \chi_{02}), \quad \chi \in (-\chi_{02}, 0), \quad \text{respectively,} \\
\xi(\chi) &= \frac{2}{\sqrt{6\beta|1+\delta|}\sqrt{r_1^2 - \psi_M^2}} \left[\left(3\psi_M^2 + \frac{1}{r_1^2} - 4\right)\chi \right. \\
&\quad \pm \left(\frac{r_2^2 - \psi_M^2}{r_2^2 \psi_M^2}\right) \Pi \left(\arcsin(\mathrm{sn}(\chi, k)), \frac{r_2^2}{\psi_M^2}, k\right) \\
&\quad \left. \pm 3(r_1^2 - \psi_M^2)(E(\arcsin(\mathrm{sn}(\chi, k)), k)) - \mathrm{dn}(\chi, k)\mathrm{tn}(\chi, k)) \right],
\end{aligned} \tag{3.4}$$

where $k^2 = \frac{r_1^2 - r_2^2}{r_1^2 - \psi_M^2}$, $\chi_{02} = \mathrm{cn}^{-1}\left(\sqrt{\frac{r_2^2}{r_2^2 - \psi_M^2}}, k\right)$.

We notice that when $\delta \to \frac{1}{8}$, there exist two segments in two homoclinic orbits, which are close to the singular straight lines $\psi = \pm\psi_s$. Thus, on the basis of the rapid-jump property of the derivative near the singular straight line given by [10], two solitary wave solutions gradually become two quasi-peakon solutions. Finally, when $\delta = \frac{1}{8}$, they become one peakon solution and one anti-peakon solution.

(iii) The case of $\delta = \frac{1}{8}$ (see Figure 2(c)) The level curves defined by $H_+(\psi, y) = h_s = h_0$ contain two homoclinic orbits of system (1.9) with eight figure to the equilibrium point $E_0(0,0)$, enclosing the equilibrium points $E_1(\psi_1, 0)$ and $E_2(\psi_1, 0)$ and its symmetric point with respect to $y-$axis, as well as two straight lines $\psi = \pm\psi_s$. For system (2.1), the eight figure is not its homoclinic orbits, because $E_{s\pm}(\pm\psi_s, \pm Y_s)$ are its saddle points. Two homoclinic orbits give rise to two solitary wave solutions of system (1.9). In addition, as three boundary curves of the period annulus of the equilibrium point $E_1(\psi_1, 0)$ of system (1.9), there exists a curve triangle (the heteroclinic loop of system (2.1)), which gives rise to a peakon solution of system (1.9). It is a limit solution of a family of periodic peakons of system (1.9).

In fact, corresponding to the right homoclinic orbits, the function $G(\psi^2) = (\psi_M^2 - \psi^2)(\psi_s^2 - \psi^2)(\psi_M^2 - \psi^2)\psi^2$ in (3.2). Now (3.2) can be written as

$$\frac{1}{2}\sqrt{3\beta}\xi = \int_z^{z_M} \frac{(\frac{1}{3} - z)(1-z)dz}{\sqrt{(z_M - z)(z - \frac{1}{3})^2 z^2}} = \int_z^{z_M} \frac{(1-z)dz}{z\sqrt{z_M - z}},$$

where $z_M = \psi_M^2$. Thus, we obtain the following parametric representation of the bright solitary wave solution (see Figure 4(a)):

$$\begin{aligned} \psi(\chi) &= \psi_M \operatorname{sech}(\chi), \\ \xi(\chi) &= \frac{4}{\psi_M\sqrt{3\beta}}\left[\chi - \psi_M^2 \tanh(\chi)\right]. \end{aligned} \tag{3.5}$$

Write that $\chi_{03} = \operatorname{arccosh}\left(\frac{\psi_M}{\psi_s}\right)$. Then, peakon solution of system (1.9) has the following parametric representation (see Figure 4(b)):

$$\begin{aligned} \psi(\chi) &= \psi_M \operatorname{sech}(\chi), \quad \chi \in (-\infty, \chi_{03}), \quad \chi \in (\chi_{03}, \infty), \quad \text{respectively}, \\ \xi(\chi) &= \frac{4}{\psi_M\sqrt{3\beta}}\left[\chi - \psi_M^2 \tanh(\chi)\right]. \end{aligned} \tag{3.6}$$

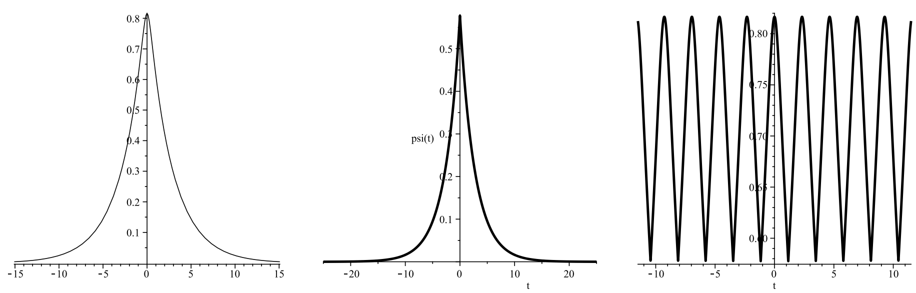

(a) Solitary wave defined by (3.5) (b) Peakon solution (c) Periodic peakon

Figure 4. Solitary wave, peakon and periodic peakon of system (1.9) given by $H_+(\psi, y) = h_s$

Corresponding to the right arch enclosing the equilibrium point $E_2(\psi_2, 0)$, the periodic peakon solution (see Figure 4(c)) has the following parametric representation (one period):

$$\begin{aligned} \psi(\chi) &= \psi_M \operatorname{sech}(\chi), \quad \chi \in (-\chi_{03}, 0), \quad \chi \in (0, \chi_{03}), \quad \text{respectively}, \\ \xi(\chi) &= \frac{4}{\psi_M\sqrt{3\beta}}\left[\chi - \psi_M^2 \tanh(\chi)\right]. \end{aligned} \tag{3.7}$$

It is very interesting that when $\delta = \frac{1}{8}$, we find the coexistence of peakon and solitary wave solution defined by (3.6) and (3.5), respectively.

(iv) The case of $\frac{13}{32} < \delta < \frac{1}{54}(-19 + 13\sqrt{13})$. The level curves defined by $H_+(\psi, y) = h_1$ contain two homoclinic orbits to the equilibrium point $E_1(\psi_1, 0)$ and its symmetric point with respect to $y-$axis, enclosing the equilibrium point $E_2(\psi_2, 0)$ and its symmetric point with respect to $y-$axis, respectively. In addition, there exist open stable manifold and unstable manifold of $E_1(\psi_1, 0)$ and its symmetric point, as well as two open curves which tend to the singular straight line $\psi = \pm\frac{1}{\sqrt{3}}$ when $|y| \to \infty$ (see Figure 2(d)).

Corresponding to the right homoclinic orbits, the function $G(\psi^2) = (\psi_M^2 - \psi^2)(\psi^2 - \psi_1^2)^2(\psi^2 - \psi_l^2)$ in (3.2). Now, (3.2) can be written as

$$\sqrt{6\beta|1+\delta|}\xi = \int_z^{z_M} \frac{(3z-1)(1-z)dz}{(z-z_1)\sqrt{(z_M - z)(z - z_l)z}},$$

where $z_M = \psi_M^2, z_l = \psi_l^2, z_1 = \psi_1^2$. Thus, we obtain the following parametric representation of the bright solitary wave solution:

$$\begin{aligned}
\psi(\chi) &= \left(\psi_M^2 - (\psi_M^2 - \psi_l^2)\mathrm{sn}^2(\chi, k)\right)^{\frac{1}{2}}, \quad \chi \in (-\chi_{04}, 0), \quad \chi \in (0, \chi_{04}), \text{ respectively,} \\
\xi(\chi) &= \tfrac{2}{\psi_M\sqrt{6\beta(1+\delta)}} \left[(4 - 3\psi_1^2)\chi \mp 3\psi_M^2 E(\arcsin(\mathrm{sn}(\chi, k)), k)\right. \\
&\quad \left. \mp \tfrac{(3\psi_1^2-1)(\psi_1^2-1)}{\psi_M^2-\psi_1^2} \Pi\left(\arcsin(\mathrm{sn}(\chi, k)), \tfrac{\psi_M^2-\psi_l^2}{\psi_M^2-\psi_1^2}, k\right)\right],
\end{aligned} \tag{3.8}$$

where $k^2 = 1 - \frac{\psi_l^2}{\psi_M^2}$, $\chi_{04} = \mathrm{sn}^{-1}\left(\sqrt{\frac{\psi_M^2-\psi_1^2}{\psi_M^2-\psi_l^2}}, k\right)$.

Considering the case of $\psi \geq 0$, we obtain the following theorem.

Theorem 3.1. *For a given $\beta > 0$, the following conclusions hold:*

(1) When $-\frac{1}{54}(19 + 13\sqrt{13}) < \delta < -1$, corresponding to the homoclinic orbit defined by $H_+(\phi, y) = h_3$, there exists a dark solitary wave solution of system (1.9) *given by* (3.3).

(2) When $0 < \delta < \frac{1}{8}$, corresponding to the homoclinic orbit defined by $H_+(\phi, y) = h_0$, there exists a bright solitary wave solution of system (1.9) *given by* (3.4).

(3) When $\delta = \frac{1}{8}$, corresponding to the homoclinic orbit defined by $H_+(\phi, y) = h_0 = h_s$, system (1.9) *has a bright solitary wave solution given by* (3.5)*, a peakon solution given by* (3.6) *and a periodic peakon solution given by* (3.7).

(4) When $\frac{13}{32} < \delta < \frac{1}{54}(-19 + 13\sqrt{13})$, corresponding to the homoclinic orbit defined by $H_+(\phi, y) = h_1$, there exists a bright solitary wave solution of system (1.9) *given by* (3.8).

3.2. Exact periodic wave solutions and periodic peakon solutions determined by system (1.9)

We see from Figure 1 that the level curves defined by $H_+(\psi, y) = h_s$ have the following graphs shown in Figure 5(a)-(d).

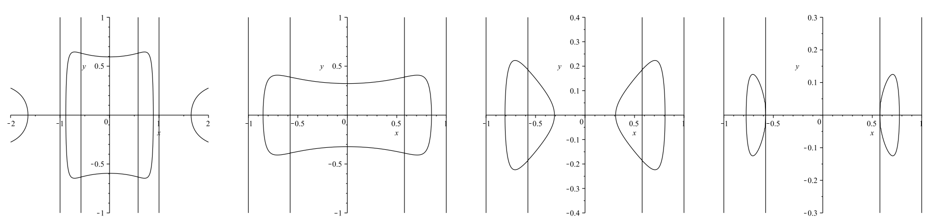

(a) $-\infty < \delta < -1, h = h_s$. (b) $-1 \leq \delta < \frac{1}{8}, h = h_s$. (c) $\frac{1}{8} < \delta < \frac{13}{32}, h = h_s$. (d) $\delta = \frac{13}{32}, h = h_s = h_1$.

Figure 5. Some level curves of system (1.9) defined by $H_+(\psi, y) = h_s$

(i) The case of $-\infty < \delta < -1, h = h_s$ (see Figure 5(a)). The level curves defined by $H_+(\psi, y) = h_s$ contain a large heteroclinic loop of system (2.1) connecting the equilibrium point $E_{s\pm}(\pm\psi_s, \pm Y_s)$ and its symmetric point with respect to $y-$axis, enclosing the equilibrium points $E_1(\psi_1, 0)$, $E_2(\psi_2, 0)$ and their symmetric points with respect to $y-$axis, respectively. In addition, there exist two open curves passing through the points $(\pm\psi_L, 0)$. Now, the function $G(\psi^2) = (\psi_L^2-\psi^2)(\psi^2-\psi_s^2)^2(\psi_M^2-\psi^2)$ in (3.2). Thus, (3.2) can be written as

$$\frac{1}{3}\sqrt{6\beta|1+\delta|}\xi = \int_z^{z_M} \frac{(1-z)dz}{\sqrt{(z_L-z)(z_M-z)z}},$$

where $z_M = \psi_M^2, z_L = \psi_L^2$. Hence, we obtain the following parametric representations of periodic solutions of system (1.9).

(1) Corresponding to the large loop, we have a periodic wave solution:

$$\begin{aligned} \psi(\chi) &= \mp\left(\psi_L^2 - \tfrac{(\psi_L^2-\psi_M^2)}{\mathrm{dn}^2(\chi,k)}\right)^{\frac{1}{2}}, \qquad \chi \in (-K(k), K(k)), \\ \xi(\chi) &= \tfrac{6}{\psi_L\sqrt{6\beta|1+\delta|}}\left[(1-\psi_L^2)\chi + (\psi_L^2-\psi_M^2)\Pi\left(\arcsin(\mathrm{sn}(\chi,k)), k^2, k\right)\right], \end{aligned} \tag{3.9}$$

where $k^2 = \frac{\psi_M^2}{\psi_L^2}$.

(2) Corresponding to the arch enclosing the equilibrium points $E_2(\psi_2, 0)$ and lies in the right side of the singular straight line $\psi = \psi_s$, we have the following periodic peakon solution (see Figure 6(a)):

$$\begin{aligned} \psi(\chi) &= \left(\psi_L^2 - \tfrac{(\psi_L^2-\psi_M^2)}{\mathrm{dn}^2(\chi,k)}\right)^{\frac{1}{2}}, \qquad \chi \in (-\chi_{p1}, \chi_{p1}), \\ \xi(\chi) &= \tfrac{6}{\psi_L\sqrt{6\beta|1+\delta|}}\left[(1-\psi_L^2)\chi + (\psi_L^2-\psi_M^2)\Pi\left(\arcsin(\mathrm{sn}(\chi,k)), k^2, k\right)\right], \end{aligned} \tag{3.10}$$

where $\chi_{p1} = \mathrm{dn}^{-1}\left(\sqrt{\frac{\psi_L^2-\psi_M^2}{\psi_L^2-\psi_s^2}}, k\right)$.

(3) Corresponding to two heteroclinic obits of system (2.1), enclosing the equilibrium points $E_0(0,0)$ and lies in the area of the two singular straight lines $\psi = \pm\psi_s$, we have the following periodic peakon solution (see Figure 6(b)):

$$\begin{aligned} \psi(\chi) &= \mp\left(\psi_L^2 - \tfrac{(\psi_L^2-\psi_M^2)}{\mathrm{dn}^2(\chi,k)}\right)^{\frac{1}{2}}, \qquad \chi \in (-\chi_{p2}, \chi_{p1}), \\ \xi(\chi) &= \tfrac{6}{\psi_L\sqrt{6\beta|1+\delta|}}\left[(1-\psi_L^2)\chi + (\psi_L^2-\psi_M^2)\Pi\left(\arcsin(\mathrm{sn}(\chi,k)), k^2, k\right)\right], \end{aligned} \tag{3.11}$$

where $\chi_{p2} = \mathrm{dn}^{-1}\left(\sqrt{\frac{\psi_L^2-\psi_M^2}{\psi_L^2+\psi_s^2}}, k\right)$.

(4) Corresponding to the arch enclosing the equilibrium points $E_2(-\psi_2, 0)$ and lies in the left side of the singular straight line $\psi = -\psi_s$, we have the following periodic peakon solution (see Figure 6(c)):

$$\begin{aligned} \psi(\chi) &= -\left(\psi_L^2 - \tfrac{(\psi_L^2-\psi_M^2)}{\mathrm{dn}^2(\chi,k)}\right)^{\frac{1}{2}}, \qquad \chi \in (-\chi_{p2}, \chi_{p2}), \\ \xi(\chi) &= \tfrac{6}{\psi_L\sqrt{6\beta|1+\delta|}}\left[(1-\psi_L^2)\chi + (\psi_L^2-\psi_M^2)\Pi\left(\arcsin(\mathrm{sn}(\chi,k)), k^2, k\right)\right]. \end{aligned} \tag{3.12}$$

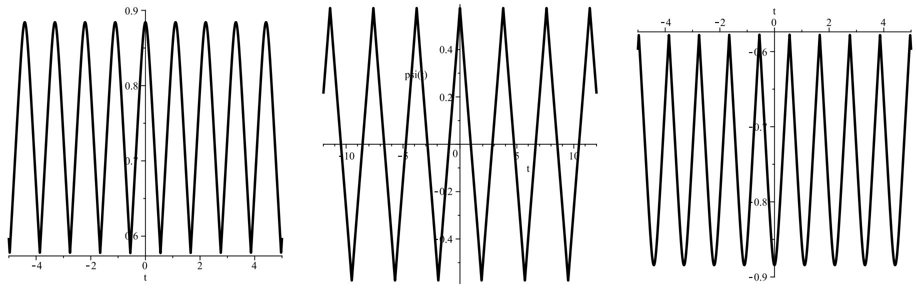

(a) Lower cusp wave (b) Zigzag curve wave (c) Upper cusp wave

Figure 6. Periodic peakon solutions of system (1.9) given by $H_+(\psi, y) = h_s$

(ii) The case of $-1 \leq \delta < \frac{1}{8}, h = h_s$ (see Figure 5(b)). The level curves defined by $H_+(\psi, y) = h_s$ contain a large heteroclinic loop of system (2.1) connecting the equilibrium point $E_{s\pm}(\pm\psi_s, \pm Y_s)$ and its symmetric point with respect to $y-$axis, enclosing the equilibrium points $E_1(\psi_1, 0)$, $E_2(\psi_2, 0)$ and their symmetric points with respect to $y-$axis, respectively (see Figure 5(b)). Now, the function $G(\psi^2) = (\psi_M^2 - \psi^2)(\psi^2 - \psi_s^2)^2(\psi^2 + \psi_I^2)$ in (3.2). Hence, (3.2) can be written as

$$\frac{1}{3}\sqrt{6\beta|1+\delta|}\xi = \int_z^{z_M} \frac{(1-z)dz}{\sqrt{(z_M - z)z(z + z_I)}},$$

where $z_M = \psi_M^2, z_I = \psi_I^2$. Thus, we obtain the following parametric representations of periodic solutions of system (1.9).

(1) Corresponding to the large loop, we have a periodic wave solution:

$$\begin{aligned} \psi(\chi) &= \psi_M \mathrm{cn}(\chi, k), \\ \xi(\chi) &= \tfrac{6}{\sqrt{6\beta(1+\delta)(\psi_M^2+\psi_I^2)}} \left[(1+\psi_I^2)\chi - (\psi_M^2 + \psi_I^2)E\left(\arcsin(\mathrm{sn}(\chi, k)), k\right)\right], \end{aligned} \tag{3.13}$$

where $k^2 = \frac{\psi_M^2}{\psi_M^2 + \psi_I^2}$.

(2) Corresponding to the arch enclosing the equilibrium points $E_2(\psi_2, 0)$ and lies in the right side of the singular straight line $\psi = \psi_s$, we have the following periodic peakon solution (see Figure 6(a)):

$$\begin{aligned} \psi(\chi) &= \psi_M \mathrm{cn}(\chi, k), \qquad \chi \in (-\chi_{p3}, \chi_{p3}), \\ \xi(\chi) &= \tfrac{6}{\sqrt{6\beta(1+\delta)(\psi_M^2+\psi_I^2)}} \left[(1+\psi_I^2)\chi - (\psi_M^2 + \psi_I^2)E\left(\arcsin(\mathrm{sn}(\chi, k)), k\right)\right], \end{aligned} \tag{3.14}$$

where $\chi_{p3} = \mathrm{cn}^{-1}\left(\frac{\psi_s}{\psi_M}, k\right)$.

(3) Corresponding to two heteroclinic obits of system (2.1), enclosing the equilibrium points $E_0(0,0)$ and lies in the area of the two singular straight lines $\psi = \pm\psi_s$, we have the following periodic peakon solution (see Figure 6(b)):

$$\begin{aligned} \psi(\chi) &= \mp\psi_M \mathrm{cn}(\chi, k), \qquad \chi \in (-K(k), \chi_{p3}), \\ \xi(\chi) &= \tfrac{6}{\sqrt{6\beta(1+\delta)(\psi_M^2+\psi_I^2)}} \left[(1+\psi_I^2)\chi - (\psi_M^2 + \psi_I^2)E\left(\arcsin(\mathrm{sn}(\chi, k)), k\right)\right], \end{aligned} \tag{3.15}$$

(4) Corresponding to the arch enclosing the equilibrium points $E_2(-\psi_2, 0)$ and lies in the left side of the singular straight line $\psi = -\psi_s$, we have the following periodic peakon solution (see Figure 6(c)):

$$\begin{aligned} \psi(\chi) &= -\psi_M \mathrm{cn}(\chi, k), \qquad \chi \in (-\chi_{p3}, \chi_{p3}), \\ \xi(\chi) \ &= \tfrac{6}{\sqrt{6\beta(1+\delta)(\psi_M^2+\psi_I^2)}} \left[(1+\psi_I^2)\chi - (\psi_M^2 + \psi_I^2 cE\left(\arcsin(\mathrm{sn}(\chi, k)), k\right)\right], \end{aligned} \tag{3.16}$$

(iii) The case of $\frac{1}{8} < \delta < \frac{13}{32}, h = h_s$ (see Figure 5(c)). The level curves defined by $H_+(\psi, y) = h_s$ contain two heteroclinic loops of system (2.1) connecting the equilibrium point $E_{s\pm}(\pm\psi_s, \pm Y_s)$ and its symmetric point with respect to $y-$axis, enclosing the equilibrium points $E_1(\psi_1, 0)$, $E_2(\psi_2, 0)$ and their symmetric points with respect to $y-$axis, respectively (see Figure 5(c)). Now, the function $G(\psi^2) = (\psi_M^2 - \psi^2)(\psi^2 - \psi_s^2)^2(\psi^2 - \psi_m^2)$ in (3.2). Thus, (3.2) can be written as

$$\frac{1}{3}\sqrt{6\beta|1+\delta|}\xi = \int_z^{z_M} \frac{(1-z)dz}{\sqrt{(z_M - z)(z - z_m)z}},$$

where $z_M = \psi_M^2, z_m = \psi_m^2$. Hence, we obtain the following parametric representations of periodic solutions of system (1.9).

(1) Corresponding to the right hrteroclinic loop, we have a periodic wave solution:

$$\begin{aligned} \psi(\chi) &= \left(\psi_M^2 - (\psi_M^2 - \psi_m^2)\mathrm{sn}^2(\chi, k)\right)^{\frac{1}{2}}, \\ \xi(\chi) \ &= \tfrac{6}{\psi_M\sqrt{6\beta(1+\delta)}} \left[\chi - \psi_M^2 E\left(\arcsin(\mathrm{sn}(\chi, k)), k\right)\right], \end{aligned} \tag{3.17}$$

where $k^2 = \frac{\psi_M^2 - \psi_m^2}{\psi_M^2}$.

(2) Corresponding to the arch enclosing the equilibrium points $E_2(\psi_2, 0)$ and lies in the right side of the singular straight line $\psi = \psi_s$, we have the following periodic peakon solution (see Figure 7(a)):

$$\begin{aligned} \psi(\chi) &= \left(\psi_M^2 - (\psi_M^2 - \psi_m^2)\mathrm{sn}^2(\chi, k)\right)^{\frac{1}{2}}, \qquad \chi \in (-\chi_{p4}, \chi_{p4}). \\ \xi(\chi) \ &= \tfrac{6}{\psi_M\sqrt{6\beta(1+\delta)}} \left[\chi - \psi_M^2 E\left(\arcsin(\mathrm{sn}(\chi, k)), k\right)\right], \end{aligned} \tag{3.18}$$

where $\chi_{p4} = \mathrm{sn}^{-1}\left(\sqrt{\frac{\psi_M^2 - \psi_s^2}{\psi_M^2 - \psi_m^2}}, k\right)$.

(3) Corresponding to the arch enclosing the equilibrium points $E_2(\psi_1, 0)$ and lies in the left side of the singular straight line $\psi = -\psi_s$, we have the following periodic peakon solution (see Figure 7(b)):

$$\begin{aligned} \psi(\chi) &= \left(\psi_M^2 - (\psi_M^2 - \psi_m^2)\mathrm{sn}^2(\chi, k)\right)^{\frac{1}{2}}, \qquad \chi \in (-K(k) - \chi_{p4}, -K(k) + \chi_{p4}). \\ \xi(\chi) \ &= \tfrac{6}{\psi_M\sqrt{6\beta(1+\delta)}} \left[\chi - \psi_M^2 E\left(\arcsin(\mathrm{sn}(\chi, k)), k\right)\right]. \end{aligned} \tag{3.19}$$

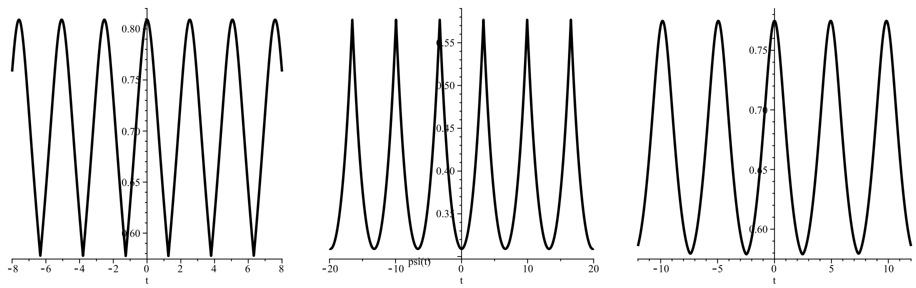

(a) Lower cusp wave (b) Upper cusp wave (c) Periodic wave

Figure 7. Periodic solutions of system (1.9) given by $H_+(\psi, y) = h_s$

(iv) The case of $\delta = \frac{13}{32}, h = h_s = h_1$. The level curves defined by $H_+(\psi, y) = h_s$ contain two oval orbits of system (2.1) contact to the two singular straight lines $\psi = \pm\psi_s$ at the point equilibrium points $(\pm\psi_s, 0)$, enclosing the equilibrium points $E_2(\psi_2, 0)$ and their symmetric points with respect to $y-$axis (see Figure 5(d)). Now, the function $G(\psi^2) = (\psi_M^2 - \psi^2)(\psi^2 - \psi_s^2)^3$ in (3.2). Thus, (3.2) can be written as

$$\frac{1}{3}\sqrt{6\beta|1+\delta|}\xi = \int_z^{z_M} \frac{(1-z)dz}{\sqrt{(z_M - z)(z - z_s)z}},$$

where $z_M = \psi_M^2, z_s = \psi_s^2$. Hence, we obtain the following parametric representations of periodic solutions of system (1.9) (see Figure 7(c)):

$$\begin{aligned} \psi(\chi) &= \left(\psi_M^2 - (\psi_M^2 - \psi_s^2)\mathrm{sn}^2(\chi, k)\right)^{\frac{1}{2}}, \\ \xi(\chi) &= \tfrac{6}{\psi_M\sqrt{6\beta(1+\delta)}}\left[\chi - \psi_M^2 E\left(\arcsin(\mathrm{sn}(\chi, k)), k\right)\right], \end{aligned} \tag{3.20}$$

where $k^2 = \frac{\psi_M^2 - \psi_s^2}{\psi_M^2}$.

To sum up, we have the following result.

Theorem 3.2. *For a given $\beta > 0$, the following conclusions hold:*

(1) When $-\infty < \delta < -1$, corresponding to the large heteroclinic loop of system (2.1) *defined by $H_+(\phi, y) = h_s$, there exists a periodic wave solution of system* (1.9) *given by* (3.9)*. In addition, system* (1.9) *has three periodic peakon solutions given by* (3.10)*,* (3.11) *and* (3.12) *which are limit solutions of three families of periodic peakon solutions defined by $H_+(\phi, y) = h$, as $h \to h_s$, respectively.*

(2) When $-1 \leq \delta < \frac{1}{8}$, corresponding to the large heteroclinic loop of system (2.1) *defined by $H_+(\phi, y) = h_s$, there exists a periodic wave solution of system* (1.9) *given by* (3.13)*. In addition, system* (1.9) *has three periodic peakon solutions given by* (3.14)*,* (3.15) *and* (3.16) *which are limit solutions of three families of periodic peakon solutions defined by $H_+(\phi, y) = h$, as $h \to h_s$, respectively.*

(3) When $\frac{1}{8} < \delta < \frac{13}{32}$, corresponding to the right heteroclinic orbit loop defined by $H_+(\phi, y) = h_s$, there exists a periodic wave solution of system (1.9) *given by* (3.17)*. In addition, system* (1.9) *has two periodic peakon solutions given by* (3.18) *and* (3.19) *which are limit solutions of two families of periodic peakon solutions defined by $H_+(\phi, y) = h$, as $h \to h_s$, respectively.*

(4) When $\delta = \frac{13}{32}$, corresponding to the oval orbit defined by $H_+(\phi, y) = h_1 = h_s$, there exists a periodic wave solution of system (1.9) *given by* (3.20)*, which is the limit solution of a family of periodic wave solutions defined by $H_+(\phi, y) = h$, as $h \to h_s$.*

3.3. Compacton solutions and bounded solutions given by system (1.9)

We first consider the open level curves in Figure 2(a) and (d). By using the "finite time interval" theorem given by [10], we know that these level curves give rise to compacton solutions of system (1.9).

(i) The case of $-\frac{1}{54}(19 + 13\sqrt{13}) < \delta < -1$ (see Figure 2(a)). The level curves defined by $H_+(\psi, y) = h_3$ contain four open curves which tend to the singular straight line $\psi = \pm\frac{1}{\sqrt{3}}$ when $|y| \to \infty$.

Corresponding to the right open orbit laying in the right side of the singular straight line $\psi = \psi_s$, the function $G(\psi^2) = (\psi_3^2 - \psi^2)^2(\psi_m^2 - \psi^2)(\psi_l^2 - \psi^2)$ in (3.2). Now, (3.2) can be written as

$$\frac{1}{3}\sqrt{6\beta|1+\delta|}\xi = \int_z^{z_l} \frac{(z - \frac{1}{3})(1-z)dz}{(z_3 - z)\sqrt{(z_m - z)(z_l - z)z}},$$

where $z_m = \psi_m^2, z_3 = \psi_3^2, z_l = \psi_l^2$. Thus, we obtain the following parametric representation of the compacton solution:

$$\begin{aligned}
\psi(\chi) =& \left(\psi_m^2 - \frac{\psi_m^2 - \psi_l^2}{\mathrm{dn}^2(\chi, k)}\right)^{\frac{1}{2}}, \qquad \chi \in (-\chi_{c1}, \chi_{c1}),\\
\xi(\chi) =& \frac{6}{\psi_m\sqrt{6\beta|1+\delta|}}\left[\left(\psi_3^2 + \psi_m^2 - \frac{4}{3} + \frac{(1-\psi_3^2)(\psi_3^2 - \frac{1}{3})}{\psi_3^2 - \psi_m^2}\right)\chi\right.\\
&- (\psi_m^2 - \psi_l^2)\Pi(\arcsin(\mathrm{sn}(\chi, k)), k^2, k)\\
&- (1-\psi_3^2)(\psi_3^2 - \frac{1}{3})\left(\frac{\psi_m^2 - \psi_l^2}{(\psi_3^2 - \psi_l^2)(\psi_3^2 - \psi_m^2)}\right)\\
&\left.\times \Pi\left(\arcsin(\mathrm{sn}(\chi, k)), \frac{(\psi_3^2 - \psi_m^2)\psi_l^2}{(\psi_3^2 - \psi_l^2)\psi_m^2}, k\right)\right],
\end{aligned} \tag{3.21}$$

where $k^2 = \frac{\psi_l^2}{\psi_m^2},\ \chi_{c1} = \mathrm{dn}^{-1}\left(\sqrt{\frac{\psi_m^2 - \psi_l^2}{\psi_m^2 - \psi_s^2}}, k\right)$.

Corresponding to the upper open orbit passing through $y-$axis, (3.2) can be written as

$$\frac{1}{3}\sqrt{6\beta|1+\delta|}\xi = \int_0^z \frac{(\frac{1}{3} - z)(1-z)dz}{(z_3 - z)\sqrt{(z_m - z)(z_l - z)z}}.$$

Thus, we obtain the following parametric representation of the compacton solution:

$$\begin{aligned}
\psi(\chi) &= \psi_l \mathrm{sn}(\chi), \qquad \chi \in (-\chi_{c2}, \chi_{c2}),\\
\xi(\chi) &= \tfrac{6}{\psi_m\sqrt{6\beta|1+\delta|}}\left[\left(\tfrac{4}{3} - \psi_3^2 - \psi_m^2\right)\chi + \psi_m^2 E(\arcsin(\mathrm{sn}(\chi, k)), k)\right.\\
&\quad \left. + \tfrac{(\psi_3^2 - 1)(\psi_3^2 - \frac{1}{3})}{\psi_3^2}\Pi\left(\arcsin(\mathrm{sn}(\chi, k)), \tfrac{\psi_l^2}{\psi_3^2}, k\right)\right],
\end{aligned} \tag{3.22}$$

where $k^2 = \frac{\psi_l^2}{\psi_m^2}$, $\chi_{c2} = \mathrm{sn}^{-1}\left(\sqrt{\frac{\psi_s}{\psi_l}}, k\right)$.

(ii) The case of $\frac{13}{32} < \delta < \frac{1}{54}(-19 + 13\sqrt{13})$ (see Figure 2(d)). The level curves defined by $H_+(\psi, y) = h_1$ contain two open curves which tend to the singular straight line $\psi = \pm\frac{1}{\sqrt{3}}$ when $|y| \to \infty$.

Corresponding to the right open orbit, the function $G(\psi^2) = (\psi_M^2 - \psi^2)(\psi_1^2 - \psi^2)^2(\psi^2 - \psi_l^2)$ in (3.2). Now, (3.2) can be written as

$$\frac{1}{3}\sqrt{6\beta|1+\delta|}\xi = \int_{z_l}^{z} \frac{(\frac{1}{3} - z)(1-z)dz}{(z_1 - z)\sqrt{(z_M - z)(z - z_l)z}},$$

where $z_M = \psi_M^2, z_l = \psi_l^2, z_1 = \psi_1^2$. Thus, we obtain the following parametric representation of the compacton solution:

$$\begin{aligned} \psi(\chi) &= \frac{\psi_l}{\mathrm{dn}(\chi,k)}, \qquad \chi \in (-\chi_{c2}, \chi_{c2}), \\ \xi(\chi) &= \frac{6}{\psi_M\sqrt{6\beta(1+\delta)}}\left[\frac{1}{3z_1}\chi - \psi_l^2\Pi(\arcsin(\mathrm{sn}(\chi,k)), k^2, k)\right. \\ &\quad \left. + \left(\frac{1}{3} - \psi_1^2\right)(1-\psi_1^2)\left(\frac{\psi_l^2}{\psi_1^2(\psi_1^2 - \psi_l^2)}\right)\Pi\left(\arcsin(\mathrm{sn}(\chi,k)), \frac{\psi_1^2(\psi_M^2 - \psi_l^2)}{\psi_M^2(\psi_1^2 - \psi_l^2)}, k\right)\right], \end{aligned} \tag{3.23}$$

where $k^2 = 1 - \frac{\psi_l^2}{\psi_M^2}$, $\chi_{c2} = \mathrm{dn}^{-1}\left(\sqrt{\frac{\psi_l}{\psi_s}}, k\right)$.

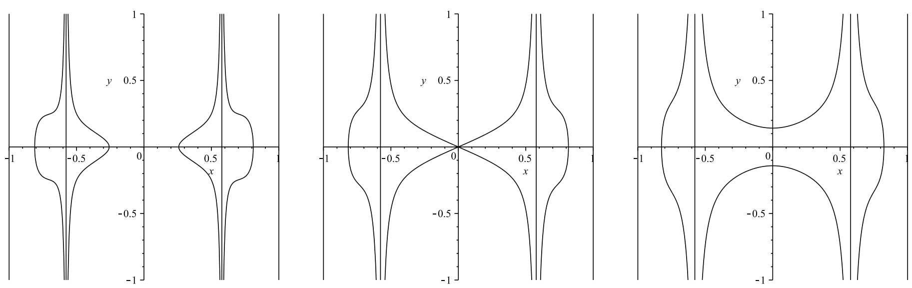

(a) $H_+(\psi, y) = h_0 - 0.01$ (b) $H_+(\psi, y) = h_0$ (c) $H_+(\psi, y) = h_0 + 0.02$

Figure 8. Some level curves of system (1.9) defined by $H_+(\psi, y) = h$

Second, we see from Figure 1 that when $\delta > \frac{1}{8}$, the level curves defined by $H_+(\psi, y) = h, h \in (h_0 - \epsilon, h_0 + \epsilon)$ have the following graphs shown in Figure 8(a)-(c). In addition, in Figure 2(a) and (d), there exist open level curves. These all open curves tend to the singular straight lines $\psi = \pm\psi_s$, as $|y| \to \infty$.

(iii) The case of $\delta > \frac{1}{8}$ (see Figure 8(b)). The level curves defined by $H_+(\psi, y) = h_0$ contain four open stable manifolds and unstable manifolds of $E_0(0, 0)$ and two open curves which tend to the singular straight line $\psi = \pm\frac{1}{\sqrt{3}}$ when $|y| \to \infty$.

In this case, the function $G(\psi^2) = \psi^2(\psi^2 + \psi_I^2)^2(\psi_L^2 - \psi^2)$ in (3.2). Corresponding to the right open orbit, (3.2) can be written as

$$\sqrt{6\beta|1+\delta|}\xi = \int_{z}^{z_L} \frac{(3z-1)(1-z)dz}{z(z+z_I)\sqrt{z_L - z}},$$

where $z_L = \psi_L^2, z_I = \psi_I^2$. Thus, we obtain the following parametric representation of the compacton solution of system (1.9):

$$\begin{aligned} &\psi(\chi) = \psi_L \mathrm{sech}(\chi), \quad \chi \in (-\chi_{c3}, \chi_{c3}), \\ &\xi(\chi) \ = \frac{3}{\sqrt{6\beta(1+\delta)}}\left[\frac{2}{3\psi_I^2\psi_L}\chi + 2\psi_L\tanh(\chi) - \frac{2(1+4\psi_I^2+3\psi_I^4)}{3\psi_I^2\sqrt{\psi_I^2+\psi_L^2}}\mathrm{arctanh}\left(\frac{\psi_L\tanh(\chi)}{\sqrt{\psi_L^2+\psi_I^2}}\right)\right], \end{aligned} \tag{3.24}$$

where $\chi_{c3} = \cosh^{-1}\sqrt{\frac{\psi_L}{\psi_s}}$.

Corresponding to the right unstable manifold to the origin $E_0(0, 0)$, (3.2) can be written as

$$\sqrt{6\beta|1+\delta|}\xi = \int_z^{z_s} \frac{(1-3z)(1-z)dz}{z(z+z_I)\sqrt{z_L - z}}.$$

We obtain the following parametric representation of the bounded solution of system (1.9):

$$\begin{aligned} &\psi(\chi) = \psi_L \mathrm{sech}(\chi), \quad \chi \in (-\infty, \chi_{c3}), \\ &\xi(\chi) \ = \frac{3}{\sqrt{6\beta(1+\delta)}}\left[\frac{2}{3\psi_I^2\psi_L}\chi + 2\psi_L\tanh(\chi) - \frac{2(1+4\psi_I^2+3\psi_I^4)}{3\psi_I^2\sqrt{\psi_I^2+\psi_L^2}}\mathrm{arctanh}\left(\frac{\psi_L\tanh(\chi)}{\sqrt{\psi_L^2+\psi_I^2}}\right) - \Psi_0\right], \end{aligned} \tag{3.25}$$

where $\Psi_0 = 2\sqrt{\psi_L^2 - \psi_s^2} - \frac{2(1+4\psi_I^2+3\psi_I^4)}{3\psi_I^2\sqrt{\psi_I^2+\psi_L^2}}\mathrm{arctanh}\left(\frac{\sqrt{\psi_L^2-\psi_s^2}}{\sqrt{\psi_L^2+\psi_I^2}}\right) + \frac{2}{3}\mathrm{arctanh}\left(\frac{\sqrt{\psi_L^2-\psi_s^2}}{\psi_L}\right)$.

The above discussion gives the following result.

Theorem 3.3. *For a given $\beta > 0$, the following conclusions hold:*

(1) When $-\frac{1}{54}(19 + 13\sqrt{13}) < \delta < -1$, corresponding to the open orbit of system (1.9) defined by $H_+(\phi, y) = h_3$ and laying in the right side of the singular straight line $\psi = \psi_s$, there exists a compacton solution of system (1.9) given by (3.21). Corresponding to the upper open orbit passing through $y-$axis, there exists a compacton solution of system (1.9) given by (3.22).

(2) When $\frac{13}{32} < \delta < \frac{1}{54}(-19 + 13\sqrt{13})$, corresponding to the open orbit of system (1.9) defined by $H_+(\phi, y) = h_1$ and laying in the left side of the singular straight line $\psi = \psi_s$, there exists a compacton solution of system (1.9) given by (3.23).

(3) When $\delta > \frac{1}{8}$, corresponding to the right unstable manifold of the origin defined by $H_+(\phi, y) = h_0$, there exists a bounded solution of system (1.9) given by (3.24). In addition, corresponding to the open orbit defined by $H_+(\phi, y) = h_0$ and laying in the right side of the singular straight line $\psi = \psi_s$, there exists a compacton solution of system (1.9) given by (3.25).

Corresponding to the level curves in Figure 8(a) and (c), we can not obtain their explicit parametric representations. By using numerical method, we obtain the graphs of the four families of compacton solutions of system (1.9) shown in Figure 9.

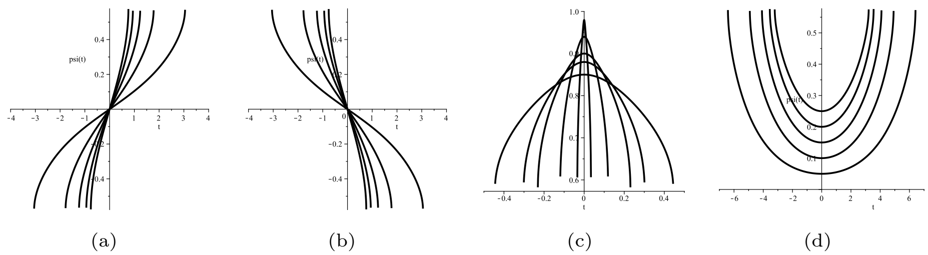

Figure 9. Compacton solution families of system (1.9) defined by $H_+(\psi, y) = h$

4. Bifurcations of phase portraits of system (1.10)

In this section, we discuss the dynamical behavior of solutions of system (1.10). We first consider the associated regular system of system (1.10) as follows:

$$\frac{d\psi}{d\zeta}=y(1-3\psi^2)(1-\psi^2)^3,\ \frac{dy}{d\zeta}=6\psi y^2(1-\psi^2)^3-\beta\psi[(1-\psi^2)^2-\psi^4+\alpha(1-\psi^2)^3],\ (4.1)$$

where $d\xi = 4(1-3\psi^2)(1-\psi^2)^3 d\zeta$. This system has the same first integral as (12). For system (4.1), the straight lines $\psi = \pm\frac{1}{\sqrt{3}}$ and $\psi = \pm 1$ is its four solutions.

Clearly, system (4.1) has an equilibrium point $E_0(0,0)$. For the other equilibrium points $E_j(\psi_j, 0)$ of system (4.1), $Z = Z_j = \psi_j^2$ satisfies the algebraic equation $f(Z) = Z^3 - 3\left(1+\frac{1}{4\alpha}\right)Z^2 + \left(3+\frac{2}{\alpha}\right)Z - \left(1+\frac{1}{\alpha}\right) = 0$, where $Z = \psi^2$. When $\delta \neq -1$, the function $f'(Z)$ has two zeros $\breve{Z}_1 = \frac{1}{6}\left[6\left(1+\frac{1}{4\alpha}\right) - \sqrt{\Delta}\right]$ and $\breve{Z}_2 = \frac{1}{6}\left[6\left(1+\frac{1}{4\alpha}\right) + \sqrt{\Delta}\right]$, where $\Delta = \frac{3(3-8\alpha)}{4\alpha^2}$. It is easy to see that

$$f(\breve{Z}_1) = -\frac{1}{144\alpha^3}\left[-18\alpha + \frac{9}{2} - 3\alpha\sqrt{\Delta} + 4\alpha^2\sqrt{\Delta} - 36\alpha^2\right],$$

$$f(\breve{Z}_2) = \frac{1}{144\alpha^3}\left[18\alpha - \frac{9}{2} - 3\alpha\sqrt{\Delta} + 4\alpha^2\sqrt{\Delta} + 36\alpha^2\right].$$

If and only if $\alpha = -\frac{1}{54}(35+13\sqrt{13})$, we have $f(\breve{Z}_1) = 0$. If and only if $\alpha = \frac{1}{54}(-35+13\sqrt{13})$, we have $f(\breve{Z}_2) = 0$. Thus, when $\alpha < -\frac{1}{54}(35+13\sqrt{13})$, or $\alpha > \frac{1}{54}(-35+13\sqrt{13})$, $f(Z)$ only has one real positive zero. When $-\frac{1}{54}(35+13\sqrt{13}) < \alpha < \frac{1}{54}(-35+13\sqrt{13})$, $f(Z)$ has three positive real zeros.

In the singular straight line $\psi = \pm\frac{1}{\sqrt{3}} = \pm\psi_s$, if $\alpha \geq -\frac{135}{96}$, there exist two equilibrium points $E_{s\pm}(\pm\psi_s, \pm Y_s)$ of system (4.1), respectively, where $Y_s = \frac{1}{24}\sqrt{135+96\alpha}$. Notice that $E_{s\pm}$ are not equilibrium points of system (1.10).

Let $M(\psi_j, y_j)$ be the coefficient matrices of the linearized systems of (4.1) at equilibrium point E_j and $J(\psi_j, y_j) = \det M_\pm(\phi_j, y_j)$. Then, one has

$$J(0,0) = -16\beta(1+\alpha), \quad J(\psi_s, Y_s) = -\frac{128}{81}\left(5 + \frac{32}{9}\alpha\right),$$

$$J(\psi_j, 0) = -\beta(1-3\psi_j^2)(1-\psi_j^2)^3\left[4(4(1-\psi_j^2)^2 - \psi_j^4 - 4\alpha(1-\psi_j^2)^3)\right.$$
$$\left. +4\psi_j(-16(1-\psi_j^2)\psi_j - 4\psi_j^3 - 24\alpha(1-\psi_j^2)\psi_j)\right].$$

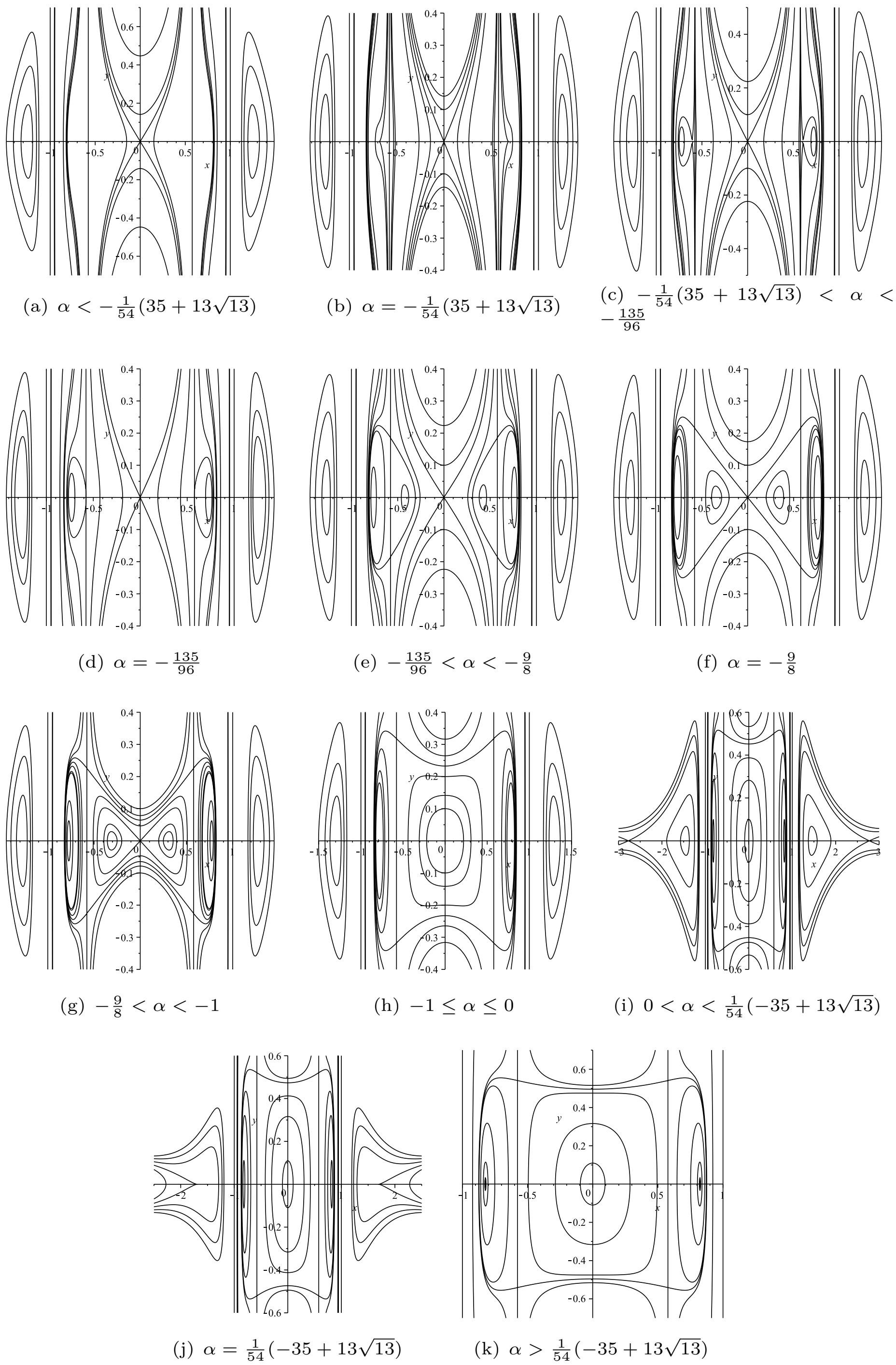

(a) $\alpha < -\frac{1}{54}(35 + 13\sqrt{13})$ (b) $\alpha = -\frac{1}{54}(35 + 13\sqrt{13})$ (c) $-\frac{1}{54}(35 + 13\sqrt{13}) < \alpha < -\frac{135}{96}$

(d) $\alpha = -\frac{135}{96}$ (e) $-\frac{135}{96} < \alpha < -\frac{9}{8}$ (f) $\alpha = -\frac{9}{8}$

(g) $-\frac{9}{8} < \alpha < -1$ (h) $-1 \leq \alpha \leq 0$ (i) $0 < \alpha < \frac{1}{54}(-35 + 13\sqrt{13})$

(j) $\alpha = \frac{1}{54}(-35 + 13\sqrt{13})$ (k) $\alpha > \frac{1}{54}(-35 + 13\sqrt{13})$

Figure 10. Bifurcations of phase portraits of system (1.10) in the (ψ, y)-phase plane

For $H_-(\psi, y) = h$ given by (1.12), write

$$h_0 = H_-(0,0) = -\frac{3}{2}\beta, \quad h_s = H_-(\psi_s, Y_s) = -\frac{1}{48}\beta(8\alpha - 63), \quad h_j = H_-(\psi_j, 0).$$

Obviously, if and only if $\alpha = -\frac{9}{8}$, we have $h_0 = h_s$.

Without loss of generality, we assume that $\beta = \frac{\omega^2}{v^2}$ is a fixed positive real number. Then, by using the above information to do qualitative analysis, we obtain the bifurcations of phase portraits of systems (1.10) and (4.1) shown in Figure 10(a)-(k).

We notice that $\alpha = -(1 + \delta)$. Hence, it is easy to see that for a given $\beta > 0$, with the change of the parameter α, the order of phase portraits in Figure 10 is just opposite with the order in Figure 1. Therefore, for system (1.10), the existence of the solitary wave solution, periodic wave solution, peakon solution, periodic peakon solution and compacton solution is similar to system (1.9). We omit the discussion for this system.

Acknowledgments

We are very grateful to our esteemed Mentor, Professor Jibin Li in the School of Mathematical Sciences, Huaqiao University, for his valuable instructions and suggestions on our paper.

References

[1] J. C. Brunelli, *The short pulse hierarchy*, Journal of mathematical physics, 2005, 46(12), 123507.

[2] J. C. Brunelli, *The bi-Hamiltonian structure of the short pulse equation*, Physics Letters A, 2006, 353(6), 475–478.

[3] P. F. Byrd and M. D. Friedman, *Handbook of Elliptic Integrals for Engineers and Scientists*, Springer, Berlin, 1971.

[4] B. Feng, *Complex short pulse and coupled complex short pulse equations*, Physica D: Nonlinear Phenomena, 2015, 297, 62–75.

[5] B. Feng, L. Ling and Z. Zhu, *Defocusing complex short-pulse equation and its multi-dark-soliton solution*, Physical Review E, 2016, 93(5), 052227.

[6] V. K. Kuetche and T. C. Kofane, *On two-loop soliton solution of the Schäfer–Wayne short-pulse equation using hirota's method and hodnett–moloney approach*, Journal of the Physical Society of Japan, 2007, 76(2), 024004–024004.

[7] J. Li, *Dynamical understanding of loop soliton solution for several nonlinear wave equations*, Science in China Series A: Mathematics, 2007, 50(6), 773–785.

[8] J. Li, *Singular nonlinear travelling wave equations: Bifurcations and exact solutions*, Science Press, Beijing, 2013.

[9] J. Li, *Variform exact one-peakon solutions for some singular nonlinear traveling wave equations of the first kind*, International Journal of Bifurcation and Chaos, 2014, 24(12), 1450160.

[10] J. Li and G. Chen, *On a class of singular nonlinear traveling wave equations*, International Journal of Bifurcation and Chaos, 2007, 17(11), 4049–4065.

[11] J. Li and Z. Qiao, *Peakon, pseudo-peakon, and cuspon solutions for two generalized camassa-holm equations*, Journal of mathematical physics, 2013, 54(12), 123501.

[12] Y. Matsuno, *Multiloop soliton and multibreather solutions of the short pulse model equation*, Journal of the Physical Society of Japan, 2007, 76(8), 084003.

[13] Y. Matsuno, *Periodic solutions of the short pulse model equation*, Journal of Mathematical Physics, 2008, 49(7), 073508.

[14] E. Parkes, *Some periodic and solitary travelling-wave solutions of the short-pulse equation*, Chaos, Solitons & Fractals, 2008, 38(1), 154–159.

[15] A. Sakovich and S. Sakovich, *The short pulse equation is integrable*, Journal of the Physical Society of Japan, 2005, 74(1), 239–241.

[16] A. Sakovich and S. Sakovich, *Solitary wave solutions of the short pulse equation*, Journal of Physics A: Mathematical and General, 2006, 39(22), L361.

[17] T. Schäfer and C. Wayne, *Propagation of ultra-short optical pulses in cubic nonlinear media*, Physica D: Nonlinear Phenomena, 2004, 196(1-2), 90–105.

[18] S. Shen, B. Feng and Y. Ohta, *From the real and complex coupled dispersionless equations to the real and complex short pulse equations*, Studies in Applied Mathematics, 2016, 136(1), 64–88.

[19] J. Song and J. Li, *Bifurcations and exact travelling wave solutions for a shallow water wave model with a non-stationary bottom surface*, Journal of Applied Analysis and Computation, 2020, 10(1), 350–360.

[20] A. Yariv and Y. Pochi, *Optical waves in crystals: propagation and control of laser radiation*, Wiley, New York, 1984.

[21] P. Yu, M. Han and Y. Bai, *Dynamics and bifurcation study on an extended lorenz system*, Journal of Nonlinear Modelling Analysis, 2019, 1(1), 107–128.

[22] Y. Zhou, J. Song and T. Han, *Solitary waves, periodic peakons, pseudo-peakons and compactons given by three ion-acoustic wave models in electron plasmas*, Journal of Applied Analysis and Computation, 2019, 9(2), 810–828.